3-Hydroxyanthranilic Acid Delays Paralysis in *Caenorhabditis elegans* Models of Amyloid-Beta and Polyglutamine Proteotoxicity

Bradford T. Hull , Kayla M. Miller , Caroline Corban , Grant Backer , Susan Sheehan , Ron Korstanje ,

George L. Sutphin *

Article

3-Hydroxyanthranilic Acid Delays Paralysis in *Caenorhabditis elegans* Models of Amyloid-Beta and Polyglutamine Proteotoxicity

Bradford T. Hull [1], Kayla M. Miller [2], Caroline Corban [3], Grant Backer [3], Susan Sheehan [3], Ron Korstanje [3] and George L. Sutphin [1,2,*]

[1] Molecular and Cellular Biology Department, University of Arizona, Tucson, AZ 85721, USA
[2] Cancer Biology Graduate Interdisciplinary Program, University of Arizona, Tucson, AZ 85721, USA
[3] The Jackson Laboratory, Bar Harbor, ME 04609, USA
[*] Correspondence: sutphin@arizona.edu

Abstract: Age is the primary risk factor for neurodegenerative diseases such as Alzheimer's and Huntington's disease. Alzheimer's disease is the most common form of dementia and a leading cause of death in the elderly population of the United States. No effective treatments for these diseases currently exist. Identifying effective treatments for Alzheimer's, Huntington's, and other neurodegenerative diseases is a major current focus of national scientific resources, and there is a critical need for novel therapeutic strategies. Here we investigate the potential for targeting the kynurenine pathway metabolite 3-hydroxyanthranilic acid (3HAA) using *Caenorhabditis elegans* expressing amyloid-beta or a polyglutamine peptide in body wall muscle, modeling proteotoxicity in Alzheimer's and Huntington's disease-related, respectively. We show that knocking down the enzyme that degrades 3HAA, 3HAA dioxygenase (HAAO) delays age-associated paralysis in both models. This effect on paralysis was independent of protein aggregation in the polyglutamine model. We also show that the mechanism of protection against proteotoxicity from HAAO knockdown is mimicked by 3HAA supplementation, supporting elevated 3HAA as the mediating event liking HAAO knockdown to delayed paralysis. This work demonstrates potential for 3HAA as a targeted therapeutic in neurodegenerative disease, though the mechanism is yet to be explored.

Keywords: metabolism; tryptophan; kynurenine; Alzheimer's disease; Huntington's disease; neurodegeneration; proteotoxicity; *Caenorhabditis elegans*

1. Introduction

Neurodegenerative diseases have become increasingly prevalent as our population has shifted to an older demographic over the last 30 years. Alzheimer's disease (AD) is now the seventh leading cause of the death in the United States and the most common form of neurodegeneration in the elderly [1]. As our cells age, a functional decline in the machinery that maintains protein homeostasis results in accumulation of damaged, misfolded, and aggregate-prone proteins [2–4]. Disruption of proteostasis is considered a hallmark of aging [5,6]. Aggregation of specific protein species is a defining feature—and is thought to be involved in pathogenesis—of age-associated neurodegenerative diseases including AD and Huntington's disease (HD) [7–12]. Current treatments for these diseases generally target symptoms (cholinergic and glutamatergic signaling in neurons in AD, huntingtin production in HD), but do not address the underlying pathology [13–15]. Hundreds of clinical trials targeting different aspects of AD, HD, and other neurodegenerative disease neuropathology—amyloid toxicity, tau toxicity, huntingtin production, oxidative stress, neuroinflammation—have failed to demonstrate efficacy. Identifying effective treatments for AD and HD is a major current focus of scientific resources, and there is a critical need for novel therapeutic strategies.

The kynurenine pathway (Figure 1) is a highly conserved metabolic pathway that converts ingested tryptophan to nicotinamide adenine dinucleotide (NAD+) [16]. Several studies have shown promise in delaying aging and age-associated decline in protein homeostasis through inhibition of tryptophan degradation via the kynurenine pathway. In the roundworm *Caenorhabditis elegans*, proteotoxicity is commonly modeled by expressing aggregate-prone proteins in body wall muscle, which causes accumulation of muscle protein aggregates and accelerated paralysis with age [17,18]. van der Goot et al. [19] reported that knockdown of the gene *tdo-2*, encoding the kynurenine pathway enzyme tryptophan 2,3-dioxygenase (TDO), delayed age-associated pathology in several of these models, including worms expressing human amyloid-beta (Aβ) or a 35-unit polyglutamine tract (Q35), modeling proteotoxicity in AD and HD, respectively. We validated this observation and further found that knockdown of *kynu-1*, encoding the kynurenine pathway enzyme kynureninase (KYNU) similarly delays paralysis in these models [20]. Both interventions extend lifespan in wild type animals, supporting the broader link between maintenance of protein homeostasis and aging [19,20]. We recently reported that knockdown of *haao-1*, a third kynurenine pathway gene encoding the enzyme 3-hydroxyanthranilate 3,4-dioxygenase (HAAO), increases lifespan in *C. elegans* [21]. Worms lacking *haao-1* accumulate the HAAO metabolic substrate, 3-hydroxyanthranilic acid (3HAA), and supplementing 3HAA in the growth media similarly extends lifespan [21].

Here we examine the impact of *haao-1* inhibition on Aβ and Q35 proteotoxicity in *C. elegans*. We find that *haao-1* knockdown delays paralysis in both contexts but does not prevent Q35 protein aggregation. Supplementing 3HAA similar delays paralysis. The effectiveness at delaying paralysis was also dependent on environmental temperature. We include previously published data on knockdown of *tdo-2* or *kynu-1* in these models for comparison. These results suggest that inhibition of HAAO or supplementation with 3HAA may hold potential as a clinical intervention for neurodegenerative disease.

2. Materials and Methods

2.1. C. elegans Strains and Maintenance.

The following strains were obtained from the *Caenorhabditis* Genetic Center (CGC) in the College of Biological Sciences at the University of Minnesota: *dvIs2[pCL12(unc-54/human Abeta peptide 1-42 minigene) + rol-6(su1006)]* (CL2006) and *rmIs132[unc-54p::Q35::YFP]* (AM140). We maintained worms on solid nematode growth media (NGM) seeded with *Escherichia coli* strain HT115 bacteria at 20°C as previously described [22]. Worms were age-synchronized via bleach prep and transferred to plates containing 50 μM 5-fluorodeoxyuridine (FUdR) to prevent reproduction at the L4 larval stage [22].

2.2. RNA Interference

We conducted RNA interference (RNAi) feeding assays using standard media preparation procedures [22]. RNAi feeding bacteria were obtained from the Ahringer *C. elegans* RNAi feeding library [23,24]. All RNAi plasmids were sequenced to verify the correct target sequence. All RNAi experiments were conducted on NGM containing 1 mM Isopropyl β-D-1 thiogalactopyranoside (IPTG) to activate production of RNAi transcripts and 25 μg/mL carbenicillin to select RNAi plasmids and seeded with live *E. coli* (HT115) containing RNAi feeding plasmids. Worms were raised on egg plates seeded with RNAi bacteria until the L4 larval stage, then transferred to FUdR-containing plates seeded with RNAi bacteria as described above.

2.3.3. HAA Supplementation

3HAA supplementation was achieved by adding the appropriate mass of solid 97% pure 3HAA (Sigma-Aldrich, catalog number 148776) to NGM media during preparation prior to autoclaving. Worms were raised on egg plates containing 1 mM 3HAA until the L4 larval stage, then transferred to FUdR-containing plates containing 1 mM 3HAA as described above.

2.4. Paralysis Analysis

Paralysis experiments were conducted as previously described [20,22]. Briefly, adult worms were maintained on NGM RNAi or 3HAA plates with FUdR for the duration of their lives. Animals were examined every 1-2 days (25°C) or 2-3 days (15°C) by nose- and tail-prodding with a platinum wire pick. Worms were scored as paralyzed if they were unable to move relative to the plate surface. Worms showing vulva rupture were included in all analyses and worms that fled the surface of the plate were excluded. P-values for statistical comparison of paralysis between test groups were calculated using the log rank test (via the *survdiff* function in the R "survival" package). For paralysis experiments, raw data is provided in Appendix A and summary statistics are provided in Table S1.
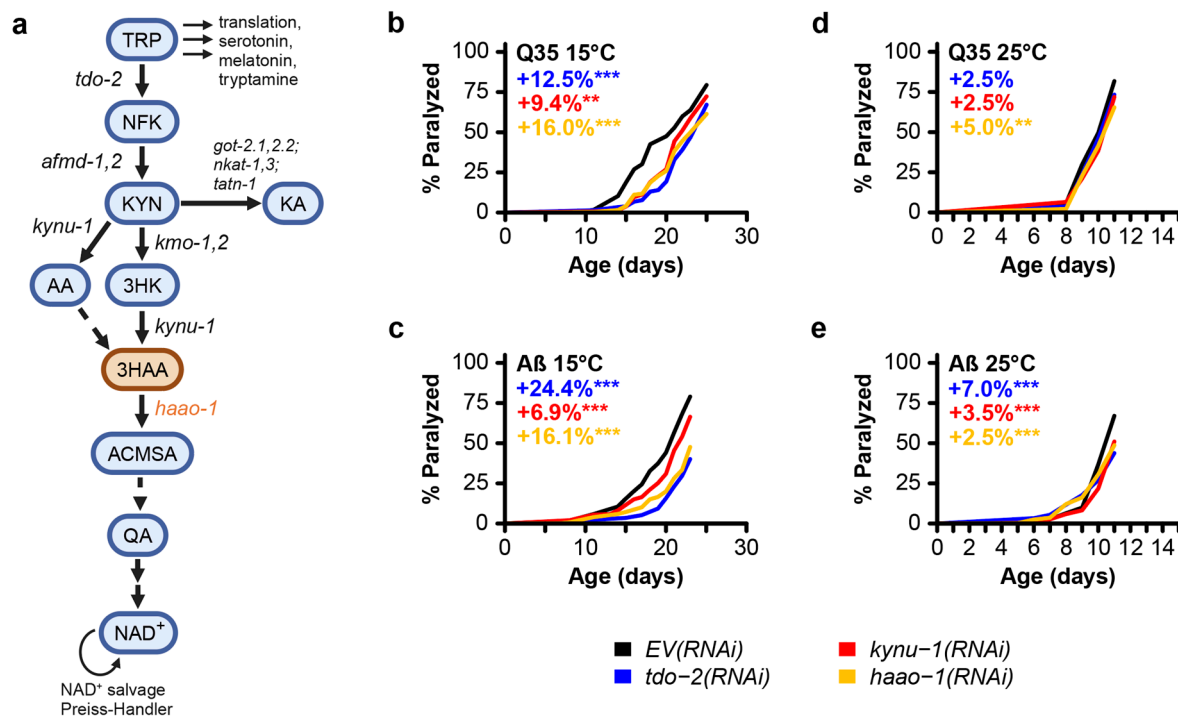
2.5. Polyglutamine Aggregate Imaging and Analysis

Polyglutamine aggregate imaging and quantification was completed as previously described [20]. Briefly, we quantified polyglutamine aggregate number and volume using 3D fluorescence microscopy of transgenic worms expressing fluorescently tagged polyglutamine repeats (Q35::YFP) at 7, 12, and 17 days of age at 15°C and 7 and 11 days of age at 25°C. At least 8 animals were examined for each RNAi at each age. Worms were immobilized using 25 nM sodium azide in M9 buffer on microscope slides with 6% agarose pads. Worms were imaged using a Leica TCS SP8 Laser Scanning Microscope equipped with a 10x objective. Z-stack images were collected for whole worms with stack spacing selected based on the Nyquist sampling theorem (minimum 2.3 images per minimum aggregate diameter). The microscope was set to capture images with resonance scanning and line averaging of 16. Images for worms that did not fit a single field of view were merged with XuvStitch version 1.8.099x64. Protein aggregates in each worm were detected and analyzed using Imaris x64 version 8.1.2. The surface tool was used to identify aggregates with thresholds for minimum fluorescence intensity and aggregate volume to ensure the analyzed surfaces were aggregates and not discrete proteins: surface = 3.0, absolute intensity = 75, seed points = 5:15, intensity > 150, volume > 45, number of voxels > 500. Aggregate volume and number were exported to R for analysis. Two-sided Welch's t-tests were used to determine significance in observed differences between target and EV RNAi at each age. For aggregate quantification experiments, raw data is provided in Appendix A and summary statistics are provided in Table S2.
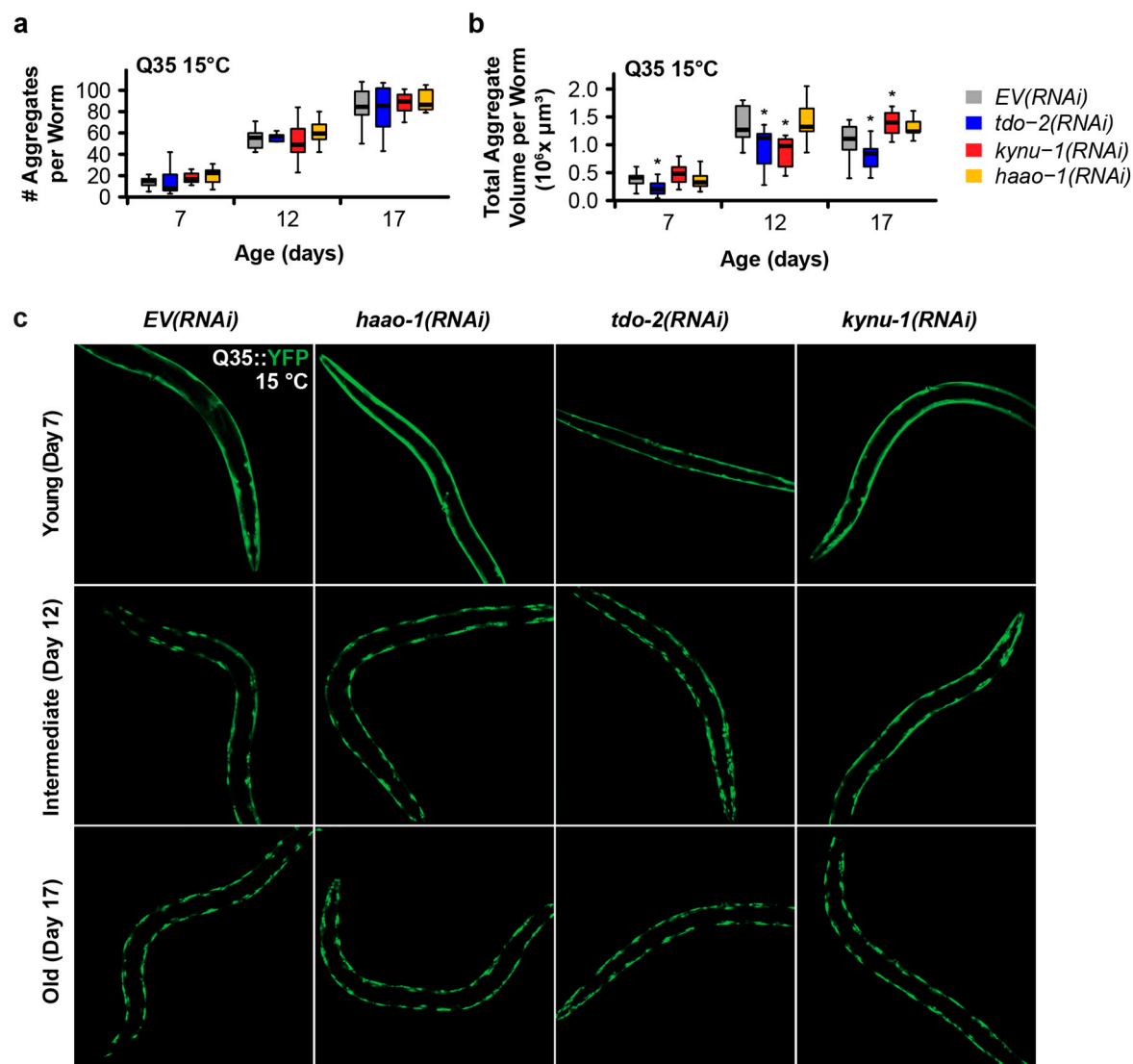
3. Results

To test the efficacy of *haao-1* disruption at improving proteotoxicity linked to neurodegeneration, we used RNAi to knockdown *haao-1* in *C. elegans* transgenically expressing polyglutamine fused to a yellow fluorescence protein (Q35::YFP) or human Aβ in body wall muscle, modeling proteotoxicity in HD and AD, respectively. We include data for both *tdo-2* and *kynu-1* knockdown for comparison [20]. Similar to previous reports for knockdown of *tdo-2* or *kynu-1* [19,20], *haao-1* knockdown delayed age-associated paralysis in worms at 15 °C (Figure 1b,c). At 25 °C, the effect was present but much smaller in both models (Figure 1d,e). These results show that *haao-1* disruption may be protective against AD- and HD-associated proteotoxicity.
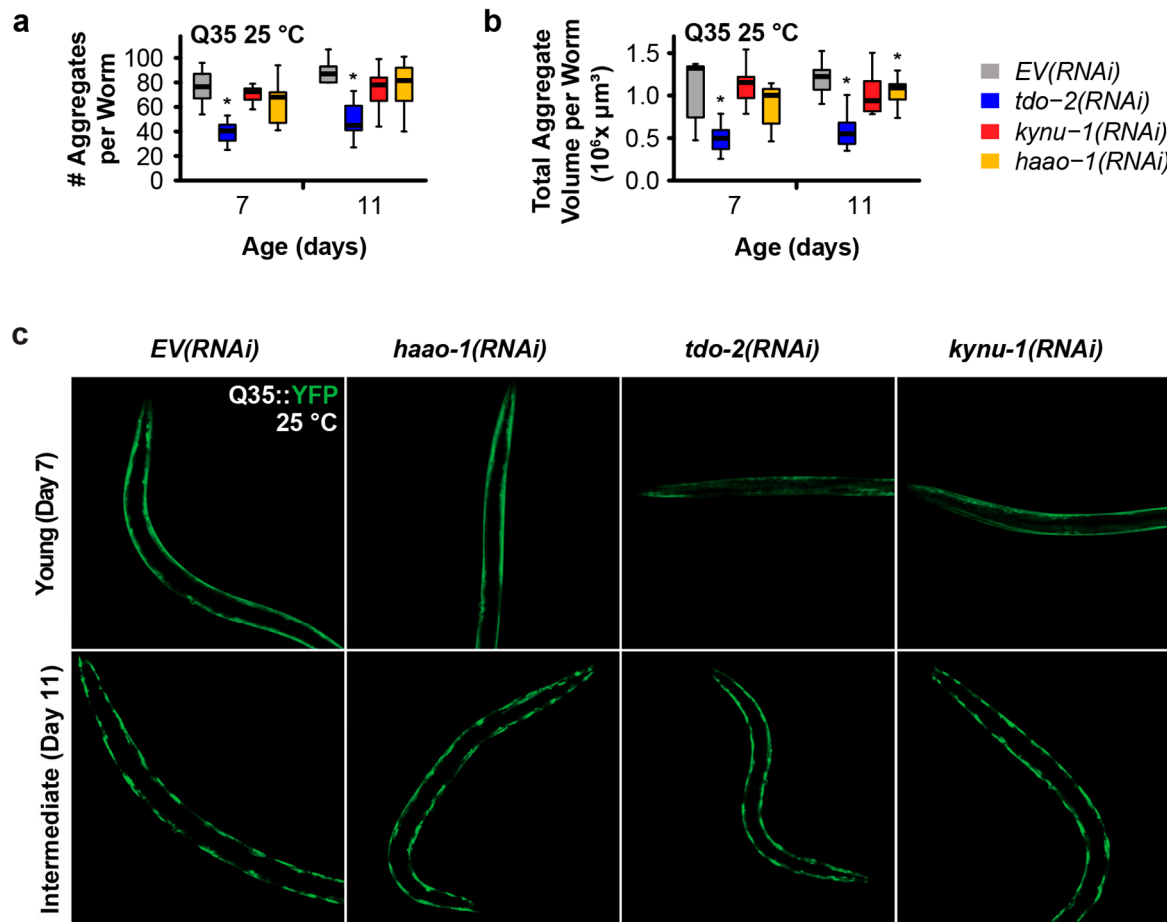
Figure 1. Knockdown of the kynurenine pathway gene *haao-1* delays paralysis in *C. elegans* models of polyglutamine and amyloid-beta proteotoxicity. (a) Schematic of the kynurenine pathway in *C. elegans*. Knockdown of *haao-1* substantially delayed age-associated pathology in *C. elegans* expressing either (b) Aβ or (c) a 35-unit polyglutamine tract (Q35) in body wall muscle at 15 °C to a similar degree as previously reported knockdown of *tdo-2* or *kynu-1* [20]. Knockdown of *haao-1* slightly delayed age-associated pathology in *C. elegans* expressing either (b) Aβ or (c) a Q35 in body wall muscle at 25 °C to a similar degree as previously reported knockdown of *tdo-2* or *kynu-1* [20]. Colored numbers indicate the percent change in mean age of paralysis vs. *EV(RNAi)*. * p < 0.05, p < 0.01, p < 0.001 for log rank test vs. *EV(RNAi)*.

We next investigated whether the mechanism of delayed paralysis in Q35::YFP worms might be a consequence of inhibition of Q35 protein aggregate formation, a hallmark of HD. We used confocal microscopy to quantify the number and size of Q35::YFP aggregates at different ages for worms cultured at a both 15 °C and 25 °C. *haao-1* knockdown did not affect either the number or volume of protein aggregates at either 15 °C (Figure 2) or 25 °C (Figure 3), with the exception of a small but significant reduction in aggregate volume at 25 °C in 11-day-old worms (Figure 3b). This is in contrast to our previously reported observation that *tdo-2(RNAi)* can reduce the number of aggregates 25 °C (Figure 3a) and aggregate volume at both 15 °C (Figure 2b) and 25 °C (Figure 3b), and that *kynu-1(RNAi)* can reduced mid-life aggregate volume at 15 °C (Figure 2b) [20]. This suggests that the protective effects of *haao-1* knockdown against polyglutamine toxicity are independent of protein aggregation.
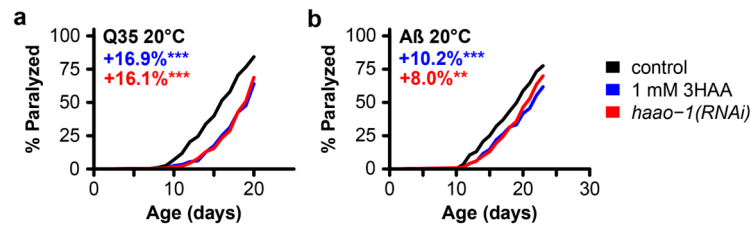
Figure 2. Knockdown of *haao-1* does not prevent polyglutamine aggregation at 15 °C. (a) *haao-1* knockdown did not affect the number YFP labeled muscle polyglutamine (Q35::YFP) protein aggregates at 15 °C, similar to our previous report for knockdown of *tdo-2* or *kynu-1* [20]. (b) *haao-1* knockdown did not affect the volume of Q35::YFP protein aggregates at 15 °C, unlike our previous report for knockdown of *tdo-2*, which reduced Q35::YFP aggregate volume at all ages examined, or *kynu-1*, which reduced Q35::YFP volume in mid-life [20]. (c) Representative images of Q35::YFP aggregation in each test group and age at 15 °C. * p < 0.05 for two-sided Welch's t test vs. age-matched *EV(RNAi)*.

Figure 3. Knockdown of *haao-1* does not prevent polyglutamine aggregation at 25 °C. (a) *haao-1* knockdown did not affect the number YFP labeled muscle polyglutamine (Q35::YFP) protein aggregates at 25 °C, similar to our previous report for knockdown of *kynu-1* and unlike knockdown of *tdo-2*, which reduced Q35::YFP aggregate number at all ages examined [20]. (b) *haao-1* knockdown slightly reduced the volume of Q35::YFP protein aggregates at 25 °C, unlike our previous report for knockdown of *tdo-2*, which substantially reduced Q35::YFP aggregate volume both at all ages examined, or *kynu-1*, which did not reduce Q35::YFP volume [20]. (c) Representative images of Q35::YFP aggregation in each test group and age at 25 °C. * p < 0.05 for two-sided Welch's t test vs. age-matched *EV(RNAi)*.

In earlier work, we found that the beneficial effects of *haao-1* knockdown on lifespan are mediated by increased physiological levels of the HAAO substrate metabolite 3HAA (Figure 1). Animals lacking functional *haao-1* accumulate 3HAA with age and 1 mM 3HAA supplementation in the growth media is sufficient to extend *C. elegans* lifespan to a similar degree as knockdown of *haao-1* [21]. Meek et al. [25] predicted *in silico* that 3HAA should bind human Aβ at a critical region for protein misfolding, and found *in vitro* that 3HAA prevented protein Aβ aggregation. To investigate whether 3HAA supplementation can similarly recapitulate the protective effects of *haao-1(RNAi)* against proteotoxicity in *C. elegans*, we supplemented worms expressing muscle Q35 and Aβ with 1 mM 3HAA. 1 mM 3HAA supplementation delayed age-associated paralysis to a nearly identical degree as experiment-matched worms subjected to *haao-1(RNAi)* in both Q35 (Figure 4a) and Aβ (Figure 4b) animals. This observation supports a model in which elevated physiological 3HAA mediates the protection against proteotoxicity by *haao-1* disruption.

Figure 4. 3HAA supplementation recapitulates the protective effects of *haao-1* knockdown against polyglutamine and Aβ proteotoxicity in *C. elegans*. Supplementing the growth media with 1 mM 3HAA In both Huntington's (A) and Alzheimer's (B) models, supplementation with 3HAA closely mimicked the effects of haao-1 knockdown. Colored numbers indicate the percent change in mean age of paralysis vs. control. * p < 0.05, p < 0.01, p < 0.001 for log rank test vs. *EV(RNAi)*.

4. Discussion

Here we describe a small study examining the impact of *haao-1* disruption or 3HAA supplementation on improving pathology in *C. elegans* models of AD- and HD-associated proteotoxicity. We first showed that *haao-1* knockdown delayed age-associated paralysis in worms, suggesting that *haao-1* disruption may be protective against proteotoxicity in AD and HD. We next investigated the mechanism of delayed paralysis and found that *haao-1* knockdown did not meaningfully affect either the number or volume of protein aggregates, suggesting that the protective effect of *haao-1* knockdown against polyglutamine or amyloid-beta proteotoxicity in *C. elegans* muscle is independent of protein aggregation. Finally, we showed that media supplementation with 1 mM 3HAA closely mimicked the benefit of *haao-1* knockdown on age-associated paralysis, supporting a model in which protection against proteotoxicity by *haao-1* disruption is mediated by elevated physiological 3HAA.

These observations suggest that *haao-1* disruption likely acts to reduce proteotoxicity via a mechanism that is at least partially distinct from both *tdo-2* and *kynu-1* because (1) *haao-1* disruption appears to be acting through 3HAA, which is not elevated by disruption of either *tdo-2* or *kynu-1* [20,21] and (2) *haao-1* disruption does not impact Q35::YFP aggregate size or volume, while disruption of both aggregate number or volume in at least one context. This leaves open that possibility that these interventions act via both common mechanisms (such as reducing production downstream metabolites) and distinct mechanisms (with *haao-1* knockdown elevating 3HAA and *tdo-2* and *kynu-1* acting via a separate mechanism). Lifespan extension from disruption of *tdo-2*, *kynu-1*, and *haao-1* was partially dependent on different combinations of established aging pathways [20,21]. Evidence presented by van der Goot et al. [19] suggests that the protection of *tdo-2* knockdown against pathology in a *C. elegans* model of alpha-synuclein proteotoxicity (modeling Parkinson's disease) may be mediated by elevated physiological levels of tryptophan. These observations provide guidance for future detailed mechanistic studies of the broader mechanisms mediating the protection of kynurenine pathway interventions against proteotoxicity.

The role of 3HAA in neurodegenerative disease has only been explored in a few small studies. Meek et al. [25] showed *in silico* that 3HAA was capable of binding to and preventing misfolding of β-amyloid in an energetically favorable reaction. Other groups have found evidence linking 3HAA to improved prognosis and survival from spinal cord injury [26,27] and represses pro-inflammatory signaling and behavior of innate immune cells [28–33], including both astrocytes and microglia [34]. Parrott et al. [35] found that *Haao* knockout mice were protected against behavioral despair induced by lipopolysaccharide (LPS)-induced inflammation. Together, these studies suggest that elevating 3HAA may have specific benefits in preventing Aβ aggregation in AD and broader benefits in neurodegenerative disease by reducing neuroinflammation.

Quinolinic acid (QA), another metabolite of the kynurenine pathway which is created from 3HAA by HAAO (Figure 1a), has been described as an endogenous neurotoxin produced in active microglia and implicated in several human neurological diseases, including AD and HD [36–38]. Tau, an endogenous microtubule-associated protein whose phosphorylation and subsequent aggregation

is considered a pathological hallmark of AD, has been shown to have elevated phosphorylation levels in the presence of QA [39]. QA has also been proposed to modulate excitotoxic neuronal death in HD [40]. Combined, this evidence suggests that HAAO disruption may be doubly beneficial for treatment of neurodegenerative disease pathogenesis in both increasing 3HAA and decreasing QA.

In summary, in this study we use *C. elegans* to investigate the benefits of HAAO disruption in preventing AD- and HD-associated proteotoxicity. We note that, while our results are positive, there are limitations with these proteotoxicity models. First, these models express Q35 or Aβ in body wall muscle instead of neurons, a distinct cellular context from the proteotoxicity that occurs in neurodegenerative disease. Second, *C. elegans* while *C. elegans* do have cells that carry out analogous roles to the mammalian innate immune system in mammals and share many conserved immune signaling pathways with mammals, they lack many elements of mammalian immunity, including an analogous adaptive immune system. Third, the Q35 polyglutamine repeat model of HD disease mimics the polyglutamine expansion in the huntingtin gene that causes human HD but does not contain the full huntingtin gene. This limits strong interpretation of these data with respect to the impact of 3HAA and HAAO in human AD and HD. However, this study and the related literature discussed above motivates future detailed mechanistic studies of 3HAA supplementation and HAAO inhibition in worm models of neuronal Aβ and polyglutamine, which have a more subtle pathology than the muscle transgenic strains used in this study, and in preclinical rodent models.

Data Availability Statement: Raw data for paralysis and aggregate quantification are provided in Appendix A. Raw images for Q35::YFP aggregation are available for download at: https://omero.jax.org/webclient/?show=project-1601.

Appendix A

This appendix contains raw data for paralysis, aggregate number, and aggregate volume.

References

1. Xu, J.; Murphy, S.L.; Kochanek, K.D.; Arias, E. *Mortality in the United States, 2021*; CDC: NCHS Data Brief, No. 456, 2022;

2. Hipp, M.S.; Kasturi, P.; Hartl, F.U. The Proteostasis Network and Its Decline in Ageing. *Nat. Rev. Mol. Cell Biol.* **2019**, *20*, 421–435. https://doi.org/10.1038/s41580-019-0101-y.

3. Labbadia, J.; Morimoto, R.I. The Biology of Proteostasis in Aging and Disease. *Annu. Rev. Biochem.* **2015**, *84*, 435–464. https://doi.org/10.1146/annurev-biochem-060614-033955.

4. Taylor, R.C.; Dillin, A. Aging as an Event of Proteostasis Collapse. *Cold Spring Harb. Perspect. Biol.* **2011**, *3*, a004440. https://doi.org/10.1101/cshperspect.a004440.

5. López-Otín, C.; Blasco, M.A.; Partridge, L.; Serrano, M.; Kroemer, G. The Hallmarks of Aging. *Cell* **2013**, *153*, 1194–1217. https://doi.org/10.1016/j.cell.2013.05.039.

6. López-Otín, C.; Blasco, M.A.; Partridge, L.; Serrano, M.; Kroemer, G. Hallmarks of Aging: An Expanding Universe. *Cell* **2023**, *186*, 243–278. https://doi.org/10.1016/j.cell.2022.11.001.

7.   Bates, G.P.; Dorsey, R.; Gusella, J.F.; Hayden, M.R.; Kay, C.; Leavitt, B.R.; Nance, M.; Ross, C.A.; Scahill, R.I.; Wetzel, R.; et al. Huntington Disease. *Nat. Rev. Dis. Primer* **2015**, *1*, 15005. https://doi.org/10.1038/nrdp.2015.5.

8.   Irvine, G.B.; El-Agnaf, O.M.; Shankar, G.M.; Walsh, D.M. Protein Aggregation in the Brain: The Molecular Basis for Alzheimer's and Parkinson's Diseases. *Mol. Med.* **2008**, *14*, 451–464. https://doi.org/10.2119/2007-00100.Irvine.

9.   Knopman, D.S.; Amieva, H.; Petersen, R.C.; Chételat, G.; Holtzman, D.M.; Hyman, B.T.; Nixon, R.A.; Jones, D.T. Alzheimer Disease. *Nat. Rev. Dis. Primer* **2021**, *7*, 33. https://doi.org/10.1038/s41572-021-00269-y.

10.   Masters, C.L.; Simms, G.; Weinman, N.A.; Multhaup, G.; McDonald, B.L.; Beyreuther, K. Amyloid Plaque Core Protein in Alzheimer Disease and Down Syndrome. *Proc. Natl. Acad. Sci. U. S. A.* **1985**, *82*, 4245–4249. https://doi.org/10.1073/pnas.82.12.4245.

11.   Masters, C.L.; Bateman, R.; Blennow, K.; Rowe, C.C.; Sperling, R.A.; Cummings, J.L. Alzheimer's Disease. *Nat. Rev. Dis. Primer* **2015**, 15056. https://doi.org/10.1038/nrdp.2015.56.

12.   Scherzinger, E.; Lurz, R.; Turmaine, M.; Mangiarini, L.; Hollenbach, B.; Hasenbank, R.; Bates, G.P.; Davies, S.W.; Lehrach, H.; Wanker, E.E. Huntingtin-Encoded Polyglutamine Expansions Form Amyloid-like Protein Aggregates in Vitro and in Vivo. *Cell* **1997**, *90*, 549–558. https://doi.org/10.1016/s0092-8674(00)80514-0.

13.   Andhale, R.; Shrivastava, D. Huntington's Disease: A Clinical Review. *Cureus* **2022**, *14*, e28484. https://doi.org/10.7759/cureus.28484.

14.   Huang, L.-K.; Kuan, Y.-C.; Lin, H.-W.; Hu, C.-J. Clinical Trials of New Drugs for Alzheimer Disease: A 2020–2023 Update. *J. Biomed. Sci.* **2023**, *30*, 83. https://doi.org/10.1186/s12929-023-00976-6.

15.   Wild, E.J.; Tabrizi, S.J. Therapies Targeting DNA and RNA in Huntington's Disease. *Lancet Neurol.* **2017**, *16*, 837–847. https://doi.org/10.1016/S1474-4422(17)30280-6.

16.   Castro-Portuguez, R.; Sutphin, G.L. Kynurenine Pathway, NAD+ Synthesis, and Mitochondrial Function: Targeting Tryptophan Metabolism to Promote Longevity and Healthspan. *Exp. Gerontol.* **2020**, *132*, 110841. https://doi.org/10.1016/j.exger.2020.110841.

17.   Link, C.D. Expression of Human Beta-Amyloid Peptide in Transgenic Caenorhabditis Elegans. *Proc. Natl. Acad. Sci. U. S. A.* **1995**, *92*, 9368–9372.

18.   Morley, J.F.; Brignull, H.R.; Weyers, J.J.; Morimoto, R.I. The Threshold for Polyglutamine-Expansion Protein Aggregation and Cellular Toxicity Is Dynamic and Influenced by Aging in Caenorhabditis Elegans. *Proc. Natl. Acad. Sci. U. S. A.* **2002**, *99*, 10417–10422. https://doi.org/10.1073/pnas.152161099.

19.   van der Goot, A.T.; Zhu, W.; Vazquez-Manrique, R.P.; Seinstra, R.I.; Dettmer, K.; Michels, H.; Farina, F.; Krijnen, J.; Melki, R.; Buijsman, R.C.; et al. Delaying Aging and the Aging-Associated Decline in Protein Homeostasis by Inhibition of Tryptophan Degradation. *Proc. Natl. Acad. Sci.* **2012**, *109*, 14912–14917. https://doi.org/10.1073/pnas.1203083109.

20.   Sutphin, G.L.; Backer, G.; Sheehan, S.; Bean, S.; Corban, C.; Liu, T.; Peters, M.J.; van Meurs, J.B.J.; Murabito, J.M.; Johnson, A.D.; et al. Caenorhabditis Elegans Orthologs of Human Genes Differentially Expressed with Age Are Enriched for Determinants of Longevity. *Aging Cell* **2017**, *16*, 672–682. https://doi.org/10.1111/acel.12595.

21.   Dang, H.; Castro-Portuguez, R.; Espejo, L.; Backer, G.; Freitas, S.; Spence, E.; Meyers, J.; Shuck, K.; Gardea, E.A.; Chang, L.M.; et al. On the Benefits of the Tryptophan Metabolite 3-Hydroxyanthranilic Acid in Caenorhabditis Elegans and Mouse Aging. *Nat. Commun.* **2023**, *14*, 8338. https://doi.org/10.1038/s41467-023-43527-1.

22.   Sutphin, G.L.; Kaeberlein, M. Measuring Caenorhabditis Elegans Life Span on Solid Media. *JoVE J. Vis. Exp.* **2009**, e1152. https://doi.org/10.3791/1152.

23.   Fraser, A.G.; Kamath, R.S.; Zipperlen, P.; Martinez-Campos, M.; Sohrmann, M.; Ahringer, J. Functional Genomic Analysis of C. Elegans Chromosome I by Systematic RNA Interference. *Nature* **2000**, *408*, 325–330. https://doi.org/10.1038/35042517.

24.   Kamath, R.S.; Fraser, A.G.; Dong, Y.; Poulin, G.; Durbin, R.; Gotta, M.; Kanapin, A.; Le Bot, N.; Moreno, S.; Sohrmann, M.; et al. Systematic Functional Analysis of the Caenorhabditis Elegans Genome Using RNAi. *Nature* **2003**, *421*, 231–237. https://doi.org/10.1038/nature01278.

25.   Meek, A.; Simms, G.; Weaver, D. Searching for an Endogenous Anti-Alzheimer Molecule: Identifying Small Molecules in the Brain That Slow Alzheimer Disease Progression by Inhibition of β-Amyloid Aggregation. *J. Psychiatry Neurosci.* **2013**, *38*, 269–275. https://doi.org/10.1503/jpn.120166.

26.   Jacobs, K.R.; Lovejoy, D.B. Inhibiting the Kynurenine Pathway in Spinal Cord Injury: Multiple Therapeutic Potentials? *Neural Regen. Res.* **2018**, *13*, 2073–2076. https://doi.org/10.4103/1673-5374.241446.

27.   Yates, J.R.; Gay, E.A.; Heyes, M.P.; Blight, A.R. Effects of Methylprednisolone and 4-Chloro-3-Hydroxyanthranilic Acid in Experimental Spinal Cord Injury in the Guinea Pig Appear to Be Mediated by Different and Potentially Complementary Mechanisms. *Spinal Cord* **2014**, *52*, 662–666. https://doi.org/10.1038/sc.2014.118.

28. Berg, M.; Stenuit, B.; Ho, J.; Wang, A.; Parke, C.; Knight, M.; Alvarez-Cohen, L.; Shapira, M. Assembly of the Caenorhabditis Elegans Gut Microbiota from Diverse Soil Microbial Environments. *ISME J.* **2016**, *10*, 1998–2009. https://doi.org/10.1038/ismej.2015.253.

29. Zhang, L.; Ovchinnikova, O.; Jönsson, A.; Lundberg, A.M.; Berg, M.; Hansson, G.K.; Ketelhuth, D.F.J. The Tryptophan Metabolite 3-Hydroxyanthranilic Acid Lowers Plasma Lipids and Decreases Atherosclerosis in Hypercholesterolaemic Mice. *Eur. Heart J.* **2012**, *33*, 2025–2034. https://doi.org/10.1093/eurheartj/ehs175.

30. Fallarino, F.; Grohmann, U.; Vacca, C.; Bianchi, R.; Orabona, C.; Spreca, A.; Fioretti, M.C.; Puccetti, P. T Cell Apoptosis by Tryptophan Catabolism. *Cell Death Differ.* **2002**, *9*, 1069–1077. https://doi.org/10.1038/sj.cdd.4401073.

31. Morita, T.; Saito, K.; Takemura, M.; Maekawa, N.; Fujigaki, S.; Fujii, H.; Wada, H.; Takeuchi, S.; Noma, A.; Seishima, M. 3-Hydroxyanthranilic Acid, an L-Tryptophan Metabolite, Induces Apoptosis in Monocyte-Derived Cells Stimulated by Interferon-Gamma. *Ann. Clin. Biochem.* **2001**, *38*, 242–251. https://doi.org/10.1258/0004563011900461.

32. Lee, W.-S.; Lee, S.-M.; Kim, M.-K.; Park, S.-G.; Choi, I.-W.; Choi, I.; Joo, Y.-D.; Park, S.-J.; Kang, S.-W.; Seo, S.-K. The Tryptophan Metabolite 3-Hydroxyanthranilic Acid Suppresses T Cell Responses by Inhibiting Dendritic Cell Activation. *Int. Immunopharmacol.* **2013**, *17*, 721–726. https://doi.org/10.1016/j.intimp.2013.08.018.

33. Gargaro, M.; Vacca, C.; Massari, S.; Scalisi, G.; Manni, G.; Mondanelli, G.; Mazza, E.M.C.; Bicciato, S.; Pallotta, M.T.; Orabona, C.; et al. Engagement of Nuclear Coactivator 7 by 3-Hydroxyanthranilic Acid Enhances Activation of Aryl Hydrocarbon Receptor in Immunoregulatory Dendritic Cells. *Front. Immunol.* **2019**, *10*, 1973. https://doi.org/10.3389/fimmu.2019.01973.

34. Krause, D.; Suh, H.-S.; Tarassishin, L.; Cui, Q.L.; Durafourt, B.A.; Choi, N.; Bauman, A.; Cosenza-Nashat, M.; Antel, J.P.; Zhao, M.-L.; et al. The Tryptophan Metabolite 3-Hydroxyanthranilic Acid Plays Anti-Inflammatory and Neuroprotective Roles During Inflammation. *Am. J. Pathol.* **2011**, *179*, 1360–1372. https://doi.org/10.1016/j.ajpath.2011.05.048.

35. Parrott, J.M.; Redus, L.; Santana-Coelho, D.; Morales, J.; Gao, X.; O'Connor, J.C. Neurotoxic Kynurenine Metabolism Is Increased in the Dorsal Hippocampus and Drives Distinct Depressive Behaviors during Inflammation. *Transl. Psychiatry* **2016**, *6*, e918. https://doi.org/10.1038/tp.2016.200.

36. Espey, M.G.; Chernyshev, O.N.; Reinhard, J.F.; Namboodiri, M.A.; Colton, C.A. Activated Human Microglia Produce the Excitotoxin Quinolinic Acid. *Neuroreport* **1997**, *8*, 431–434. https://doi.org/10.1097/00001756-199701200-00011.

37. Guillemin, G.J.; Brew, B.J.; Noonan, C.E.; Takikawa, O.; Cullen, K.M. Indoleamine 2,3 Dioxygenase and Quinolinic Acid Immunoreactivity in Alzheimer's Disease Hippocampus. *Neuropathol. Appl. Neurobiol.* **2005**, *31*, 395–404. https://doi.org/10.1111/j.1365-2990.2005.00655.x.

38. Lugo-Huitrón, R.; Ugalde Muñiz, P.; Pineda, B.; Pedraza-Chaverrí, J.; Ríos, C.; Pérez-de la Cruz, V. Quinolinic Acid: An Endogenous Neurotoxin with Multiple Targets. *Oxid. Med. Cell. Longev.* **2013**, *2013*, 104024. https://doi.org/10.1155/2013/104024.

39. Rahman, A.; Ting, K.; Cullen, K.M.; Braidy, N.; Brew, B.J.; Guillemin, G.J. The Excitotoxin Quinolinic Acid Induces Tau Phosphorylation in Human Neurons. *PLoS ONE* **2009**, *4*, e6344. https://doi.org/10.1371/journal.pone.0006344.

40. Guidetti, P.; Luthi-Carter, R.E.; Augood, S.J.; Schwarcz, R. Neostriatal and Cortical Quinolinate Levels Are Increased in Early Grade Huntington's Disease. *Neurobiol. Dis.* **2004**, *17*, 455–461. https://doi.org/10.1016/j.nbd.2004.07.006.